Paper AAS 03-165

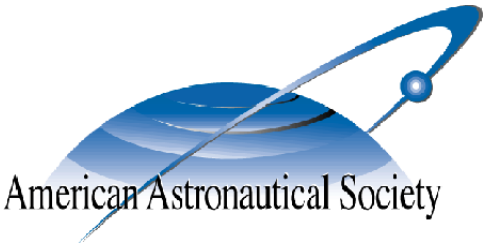

COMPARISON OF MSIS AND JACCHIA ATMOSPHERIC DENSITY MODELS FOR ORBIT DETERMINATION AND PROPAGATION

Keith Akins, Liam Healy, Shannon Coffey, Mike Picone
Naval Research Laboratory

13th AAS/AIAA Space Flight Mechanics Meeting

Ponce, Puerto Rico **9-13 February 2003**

AAS Publications Office, P.O. Box 28130, San Diego, CA 92198

AAS 03–165

Comparison of MSIS and Jacchia atmospheric density models for orbit determination and propagation

Keith A. Akins* **Liam M. Healy†** **Shannon L. Coffey‡**
J. Michael Picone§

Abstract

Two atmospheric density model families that are commonly chosen for orbit determination and propagation, Jacchia and MSIS, are compared for accuracy. The Jacchia 70 model, the MSISE-90 model, and the NRLMSISE-00 model may each be used to determine orbits over fitspans of several days and then to propagate forward. With observations kept over the propagation period, residuals may be computed and the accuracy of each model evaluated. We have performed this analysis for over 4000 cataloged satellites with perigee below 1000km for September–October 1999, and the 60 HASDM calibration satellites with a large observation set for February 2001. The purpose of this study is to form a picture of the relative merits of the drag models in a comprehensive view, using all satellites in a manner consistent with the operational practice of US space surveillance centers. A further goal is to refine this knowledge to understand the orbital parameter regions where one of the models may be consistently superior.

INTRODUCTION

Precise prediction of satellite motion in low-earth orbits requires significant knowledge of the effects of the atmospheric drag force. This force has two components which are usually difficult to ascertain: the ballistic coefficient of the satellite, and the atmospheric density at a particular point in its orbit. The problem of atmospheric density has been studied for decades, and two of the most widely-used atmospheric density models are Jacchia 70 and MSIS.

This paper presents a comparison of orbit determination and propagation results between three atmospheric density models for over 4000 satellites in low-earth orbit. These satellites represent all the unclassified satellites with perigees below 1000 km tracked by Naval Network and Space Operations Command (NNSOC, formerly Naval Space Command) in the period of September-October 1999. Further analysis is conducted using the HASDM satellite and observation data sets. This data includes 60 primary, or calibration, objects for which a very large number of observations were accumulated starting in early 2001.

*Pennsylvania State University, Aerospace Engineering, University Park, PA 16802, and Naval Research Laboratory, Code 8233, Washington, DC 20375–5355, E-mail: Keith.Akins@nrl.navy.mil.
†Naval Research Laboratory, Code 8233, Washington, DC 20375–5355. E-mail: Liam.Healy@nrl.navy.mil.
‡Naval Research Laboratory, Code 8233, Washington, DC 20375–5355.
§Naval Research Laboratory, Code 7643, Washington, DC 20375–5355.

DRAG MODELS

An important component of low-earth motion is atmospheric drag, and an important part of determining this force is knowledge of the atmospheric density. There are two major families of atmospheric density models based on empirical data collection in the 1960s, 70s, and 80s. These models provide estimates of the statistical mean temperature, total mass density, and number density of each species as a function of position, local time, universal time, and solar and geomagnetic indices. Of greatest interest to the astrodynamics community is the total mass density.

The two most widely used families of density models are *Jacchia*, based on the work of Luigi Jacchia, and *MSIS* (Mass Spectrometer — Incoherent Scatter), based on the work of Alan Hedin and collaborators (Ref. 1). The operational orbit determination community primarily uses the Jacchia 70 (J70) model (Ref. 2) while the atmospheric physics community has preferred the MSIS-class models, of which the latest is NRLMSISE-00 (N00) (Ref. 3). To compare the performance of J70 model and N00 for drag estimation, a discussion of the respective underlying observational data and the methods of generating the models is necessary. For a complete comparison, one must include the preceding MSIS-class model, MSISE-90 (M90) (Ref. 4). The two MSIS-class models extend from the ground ($z = 0\,\text{km}$) to beyond the exosphere ($z \approx 500\,\text{km}$) while the Jacchia models apply only above 90 km, unless the programmer has augmented the model at lower altitude with either the U. S. Standard Atmosphere (Ref. 5), as is done in the present analysis, or an MSIS representation, as is done in many space surveillance centers.

At thermospheric altitudes ($z > 90\,\text{km}$), all three models primarily represent parameterized solutions of the equations of diffusive equilibrium for the individual chemical constituents of the atmosphere, such as molecular nitrogen (N_2), molecular oxygen (O_2), and atomic oxygen (O). The key altitude profile parameters for thermospheric variables are the temperature and the temperature gradient near the inflection point of temperature as a function of altitude ($120 - 125\,\text{km}$), the exospheric temperature, and the total mass density and individual species densities at prescribed lower altitudes. In J70, the important parameters are temperature at 90 km and the mixing ratio $90\,\text{km} < z < 105\,\text{km}$; for the MSIS models they are composition and temperature at 120 km. These profile parameters are, in turn, decomposed into harmonic, spherical harmonic, and other terms such as the dependence of the 10.7 cm solar flux index, $F_{10.7}$, on density, each with a coefficient to be determined from data. These terms capture dependencies on characteristic temporal and spatial scales, e.g., local time (diurnal-scale tides), UT, day of year (annual-scale cycles), latitude, longitude (not explicit in J70), solar declination (not explicit in M90, N00). The generation of a model consists of computing the atmospheric densities from observations over a range of the model's parameters and then doing a nonlinear least squares fit to this density data to derive the coefficients. These coefficients then become the core of the model; they allow the estimation of density given appropriate input parameters. For a realistic model, the number of coefficients can be quite large; N00, for example, has over 2000 nonzero coefficients.

The oldest of the three models, Jacchia 70, is a fit to a set of density values derived from orbit observations of satellites covering the time period 1961–1970, falling short of a complete solar cycle. The characteristic fitspans for retrieving density were 1–4 days. Because the region of the perigee dominates the integrated drag over an orbit, Jacchia was able to assign local geophysical and temporal variables (e.g., solar zenith angle) to the density values. Jacchia then inferred the various coefficients in his analytic density model to evaluate the temperature and density profiles as functions of the subroutine arguments (time and location variables, solar index, geomagnetic index). Based on our reading of Jacchia's reports, his inferences were not the result of a formal multivariate fitting procedure, but were instead based on a filtering or separation of the individual terms (semiannual variation, diurnal variation, etc.) from the data. It has been found (Ref. 3) that J70 does not produce an acceptable representation of his set of data for particular subsets of the model arguments. Given the computing capability during the 1960s, this is neither an indictment of Jacchia's work nor a surprise. Rather, one respectfully notes the utility of J70 in operational orbital drag estimation.

In the thermosphere, $90\,\text{km} < z < 500\,\text{km}$, the MSISE-90 model is a Levenberg-Marquardt

(nonlinear least-squares) fit to a data set consisting primarily of individual species density values and temperature data, as measured by ground-based and satellite-borne systems. The vast majority of the data covers the two decades prior to 1983, but the fit excluded the total mass density derived from satellite-borne accelerometer data, and orbit determination that Jacchia used. The explicit fit to temperature and individual species density observations has rendered the MSIS-class temperature and composition estimates demonstrably superior in agreement with direct atmospheric observations to those of the Jacchia models. An important contributing factor is the use of optimal multivariate assimilation techniques in generating the model; Jacchia apparently did not do this. The atmospheric physics community has validated the model by direct measurement of the density, for example by rocket flights with mass spectrometers, primarily against short time-scale, local measurements, but has not performed similar studies of orbital drag data. These data usually resolve timescales no shorter than a day and have similarly broader spatial scales, as compared to the N00 input parameters temperature and number density. We hope that this paper will provide the first step in that process.

The primary M90 deficiency is the exclusion of data on thermospheric total mass density. The NRLMSISE-00 model now removes this deficiency by adding extensive data from orbit determination (including Jacchia's data set) and from accelerometers (Ref. 3). From the standpoint of the model generation data, the N00 model therefore represents an improvement over both M90 (total mass density) and J70 (composition and temperature). In addition, the superior representation of the temperature function should translate to superior extrapolation or interpolation of the N00 total mass density measurements to the conditions of orbital observations. On the other hand, strong temporal and spatial filtering of density estimates by the orbit determination process could mitigate any potential advantage of N00 to the operational user, depending on the orbit sampling rate and accuracy.

Our motivation in undertaking this study is primarily to see if the MSIS atmospheric model, with its better representation of the atmosphere, can improve orbit propagation over Jacchia model still widely used in the astrodynamics community. Our intent is to examine a broad spectrum of satellites, in fact all relevant satellites, and not just a few specially selected ones.

Furthermore, we anticipate, in the net few years, the capability of real-time revision of atmospheric density. Research is presently underway examining the effectiveness of modifying the N00 model with near real-time, location-specific constituent data to provide a more accurate model. Both the former LORAAS instrument, onboard the ARGOS spacecraft, and the future SSULI instrument, planned for launch on the the next DMSP spacecraft, gather UV data from limb scans of the atmosphere to determine its composition at the time and location of the scan (Ref. 6). This composition data is then applied to the base N00 model to produce a better representation of the atmosphere near where the scan was taken. The present study will provide a baseline for evaluating the effectiveness of the real-time modified MSIS models.

TEST PROCEDURE

The comparison of atmospheric drag models in the context of satellite orbits makes use of the determination of a satellite's orbit using observations, and the propagation to a time later than the range over which observations were taken. Our focus in these studies is not the initial orbit determination process (Ref. 7), but rather the orbit estimation, or differential correction, that starts with some state estimate, and provides a new estimate at some later epoch based on a new set of observations. As such, it inherently involves propagation, because these observations, the original epoch, and the new epoch, will be at varied times. As part of this propagation an accurate force model must be used, and hence the need for good knowledge of atmospheric density.

The tests conducted are designed to compare atmospheric density models by looking at how they affect orbit determination. While we do not have an absolute truth with which to compare our computed result, we can compare one model to the others and identify which is better. For each of the satellite sets used, we have a database of observations, initial elements, and the appropriate solar

indices, such as $F_{10.7}$ and the geomagnetic index a_p, for the time period in question. Other necessary data for the functioning of the orbit determination and propagation is present as well. It is important to note that the solar indices used are the retrospective final values. These are usually not available until some time after the time in question, and have been generated by Air Force Weather Agency and NOAA after extensive processing of observational data. An orbit determination on current data is different in that the value of these variables are projected into the future and therefore estimated; the final values may differ somewhat. As a result, these tests would be different from a present-time test because of the use of final values.

Abbreviation	Name
RST	Requested Stop Time
LOBST	Last Observation Before Stop Time
GPCD	General Pert Catalog Date
ESC	Epoch of Satellite in Catalog

Table 1: Important times in for orbit determination.

Before describing the test procedure, some time terminology must be introduced. The orbit determination process requires the use of several different times, and we have given each a name and an abbreviation. These are given in Table 1. First, the user must specify a final time for the orbit determination, the *requested stop time* (RST). This means that no observation after that time will be used for the orbit determination. Together with a fitspan, this determines the complete range of times over which observations may be used. The epoch of the determined vector will not be RST, but rather the time of the last observation before this time, which we call LOBST. Finally, to start the orbit determination we will need to use an element set from the NNSOC catalog; for convenience we give a date to this catalog, *general perturbations catalog date* (GPCD). More importantly, each satellite in this catalog has an epoch, which we call the *epoch of satellite in catalog* (ESC).

There are two sets of data on which the tests have been performed: all unclassified cataloged satellites with perigee below 1000 km drawn from a the set of all unclassified observations in the NNSOC (then Naval Space Command) catalog as of October 1999, which we call *lowsats*, and the HASDM calibration satellites from February 2001. The HASDM satellites were used because of the high number of available observations. The disadvantage is that these orbits, while selected to be representative of all applicable orbits, still are only a small fraction of the possible orbits affected by drag. The full catalog of objects with perigees below 1000 km was selected because these were all known satellites passing through the high drag region and therefore will show how the drag model affects operational analysis.

Both the differential correction and the propagation for this project were conducted using the Naval Research Laboratory's SPeCIAL-K orbit determination software suite (Ref. 8). This software, which is used at NNSOC, uses Special Perturbations (SP) for accurate integration and force modeling. The integration for this study was performed using an 8th-order Gauss-Jackson integrator, a 24×24 geopotential, and lunar and solar perturbations. Standard observational weighting and biasing was used, and, for the differential correction, the fitspan was defined, using standard operational algorithms, to be between 1.5 and 10 days based on the mean motion and the rate of change of mean motion of each object. SPeCIAL-K's automatic parallel processing capabilities allowed the large differential corrections to finish in approximately 4 hours. These runs were completed using 13 workers on a variety of computer platforms, including SGI, AIX and Linux.

There are several ways one might consider comparing the validity of an orbit determination process, including, of course, the atmospheric density model. The purpose in doing an orbit determination is to predict the orbit of a satellite, and as such models can be compared by their predictive power. This process is illustrated in Fig. 1. Additionally, the propagation capabilities of a model can be determined by using observations after the initial RST. With these new observations, one can predict forward and compute residuals, as is shown in Fig. 2. Finally, one can determine a new orbit one day advanced from the first correction and compare the final position with the position

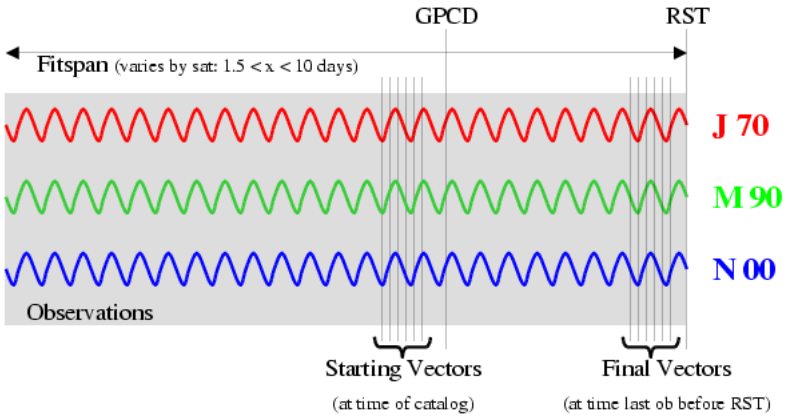

Figure 1: A schematic illustration of differential correction test.

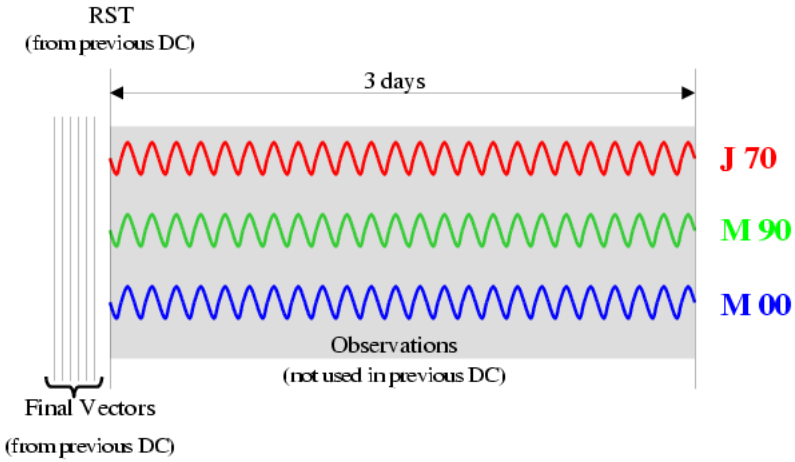

Figure 2: A schematic illustration of orbit propagation test.

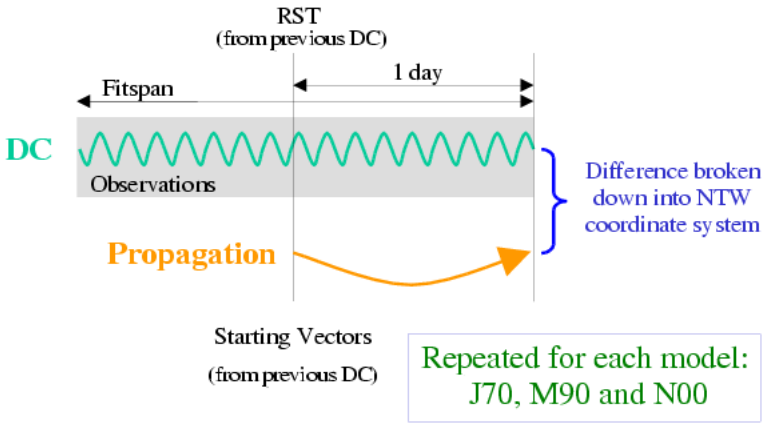

Figure 3: A schematic illustration of day-to-day test.

propagated from the first orbit determination, such as in Fig. 3. Either way, we have a reference truth based on the observations held in reserve.

INITIAL VECTOR QUALITY

When doing orbit determination by performing a differential correction, one needs an initial vector upon which to start the correction process. In the case of the tests described here, that comes from a general perturbations element set containing known orbital parameters of the satellite. It may be felt that such an element set is too inaccurate to provide convergence to the correct orbit directly, and so one may consider a process called *smoothing*. This process consists of the application of orbit determination on the initial state vector derived from the element set. By using a force model more accurate than general perturbations, including drag, it is hoped that the initial conditions will be closer to the true solution.

An important point is that smoothing will use an atmospheric density model as part of the drag force calculation. Prior to performing tests of the atmospheric model, we wish to assess the effect of smoothing. Specifically, we were concerned that we might introduce a bias in favor of the drag model used for smoothing, assuming all tests were smoothed the same way.

In principle a Newton-Raphson process, which is the essence of differential correction, should converge to the same value regardless of the starting vector, provided the starting point is in the basin of convergence (Ref. 9) for the solution. Therefore, one might assume that smoothing is an unnecessary step, and further, would not introduce any bias, presuming the basin boundaries did not change. To test this hypothesis, we performed a test we call "roughing," which is to take the vector converted from GP elements, add a random vector, and then do a differential correction. If the resulting vectors were the same or similar, one could assume this hypothesis true, and assume smoothing unnecessary but also non-biasing. The random vector would be chosen from a Gaussian distribution with a mean of zero and a standard deviation equal to the amount the vector changed in the smoothing calculation.

We chose as the test set the fifty satellites with perigee altitude below 1000 km that had the greatest number of available observations in the database from September–October 1999. Initially, the corresponding fifty element sets distributed by Naval Space Command on September 29, 1999 were converted to state vectors and these vectors were used as the starting points for the differential correction. In this test, GPCD is the day prior to RST; therefore ESC is at least 24 hours before LOBST.

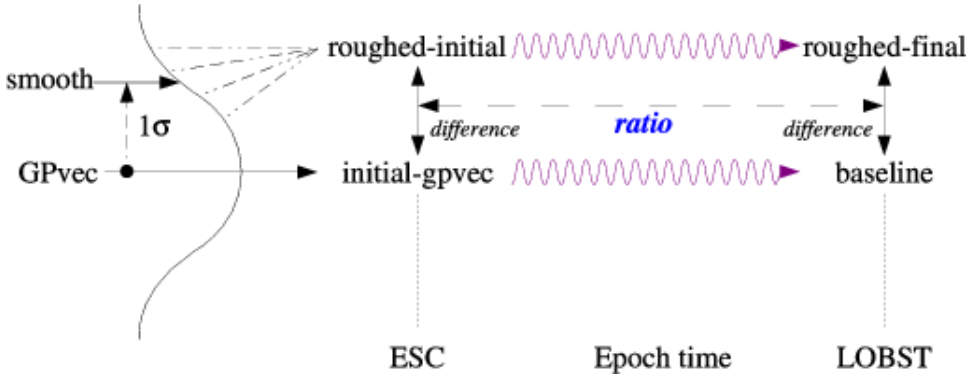

Figure 4: Roughing schematic. Once the smoothed vector has been determined, the difference between it and the GP vector is used as the standard deviation for the random generation of the roughed vector. The orbit is determined for both that and the original vector, and the ratio of the differences of the results formed.

We performed the roughing test on these satellites with the following procedure; see Fig. 4.

First, we retrieved catalog elements with a GPCD of 1999-09-29. These were converted to vectors at ESC. Alternatively, we create the "smoothed" vectors by fitting with observations prior to ESC and using a Jacchia 70 model, propagate the fit vectors to ESC. RST is 1999-09-30 00:00:00.000. Therefore, for each satellite we have two vectors at their ESC, one from the general perturbations propagation of the element set, and one from a differential correction on the observations using the element set as the initial vector, the smoothed vector. The important quantity derived from the smoothed vector is its difference from the general perturbations propagated one. This difference is used as the standard deviation in the generation of a Gaussian noise term to add to the general perturbations vector.

Orbit determination is performed on each of these two sets of vectors, with the final epoch being at LOBST with RST being 1999-10-01 00:00:00. For the position and velocity, the vector magnitude of the difference at this time between these two vectors may be computed, and a ratio formed with the corresponding vector magnitude of the difference of the roughed initial and the initial GP vector. This ratio is a figure of merit for the roughing test.

We have taken measures to make the differential correction consistent between the baseline and perturbed vector cases. First, we performed the differential correction normally on the baseline case. During such a run, there are observations that are rejected for a variety of reasons. These observations were then removed from the database for future runs, and the ability for the program to reject observations disabled. This has the effect of insuring that each baseline and perturbed case has an identical set of reasonable observations. Furthermore, we decreased the convergence tolerance of fractional weighted RMS change from the default 0.01 to 0.001. This means that solving the same orbit with different input vectors will result in more consistent results because the program quits iteration on RMS increase as well as decrease, and a decrease of tolerance makes it more likely to get through a "hump" that is often experienced where the RMS increases and then decreases before converging.

The results of this test are given in Figure 5. The bars indicate the range of ratios, and diamond indicates the mean. The results indicate that generally the ratio is quite small, less than 0.1, indicating that the baseline and the perturbed vectors all converge to essentially the same point. There are a few exceptions; notably satellite 25680, for which the ratios are rather large. This is because for the baseline case, the differential correction iteration was terminated for reasons other than convergence.

Therefore, we conclude that, within reason, perturbations of the initial vector do not affect the result of the differential correction and therefore smoothing is unnecessary. There are two caveats. First, this assumes the differential correction terminates at convergence. Second, in some cases, if observation rejection is not controlled, the set of accepted observations may be different and if so, there could be detectable differences in the resulting fit. There is no reason to believe this biases the result towards a particular drag model, however, it therefore also seems unnecessary to perform a smoothing operation in the first place.

RMS TEST

Comparing atmospheric models is difficult for a variety of reasons: there is usually no direct measurement of density, only the indirect measure from the satellite motion which involves additional unknowns; models vary in their accuracy over regions of the atmosphere and solar conditions, leading to mixed results depending on the orbit studied; and it is difficult to find a good measure of accuracy of orbits.

One way of testing the models' value to orbit propagation is to examine the residuals. Comparisons are done by examining the residual errors of both the differential correction and propagation between the models. A one-day differential correction is performed with each atmospheric model, and the epoch moved forward by the one day. The final root-mean-squared residual errors are then compared to evaluate the relative effectiveness of the particular model in a differential correction. The predictive effectiveness of the drag models is then calculated by predicting forward for three

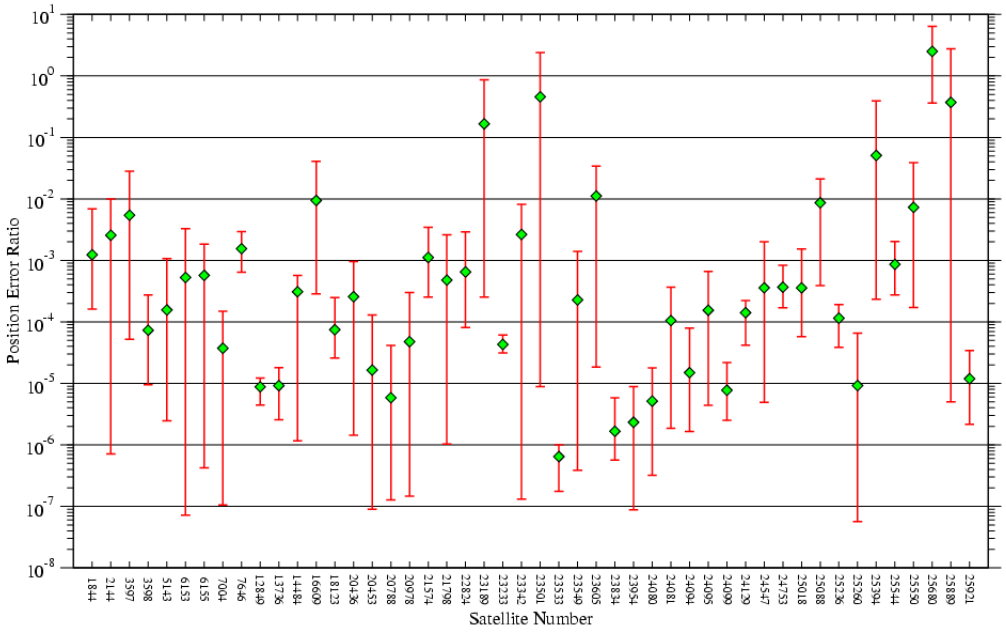

Figure 5: Ratios of final position difference to initial position difference.

days and computing the root-mean-squared residual errors at each of the known observations. In our test, we included only those satellites that updated in all cases. For the lowsats, the total number of such satellites included is 4587; for HASDM, all 60 satellites updated.

	M90	N00
lowsats DC mean	−0.00189	−0.00298
lowsats DC std. dev.	0.0913	0.0848
lowsats Prop. mean	−0.0451	−0.0325
lowsats Prop. std. dev.	0.271	0.328
HASDM DC mean	0.0170	0.0139
HASDM DC std. dev.	0.0754	0.169
HASDM Prop. mean	0.282	0.142
HASDM Prop. std. dev.	0.584	0.456

Table 2: RMS fractional change from J70 to the MSIS models.

In order to see the effect on differential correction and orbit propagation in changing the model from Jacchia 70 to both MSIS models, we have plotted the fractional change in unweighted RMS that is computed for each satellite. In Fig. 6 for differential correction and Fig. 8 for orbit propagation, these fractional changes are plotted by satellite in increasing order. With a scatter plot (Fig. 7 for differential correction and Fig. 9 for propagation) of the RMS with respect to various fit values, one may attempt to isolate certain orbits for which one or the other atmosphere model is superior. No such correlation is apparent, although some trends are discernible. The plots for the HASDM set (Figures 10– 13) are qualitatively similar. The RMS fractional change results are summarized in Table 2.

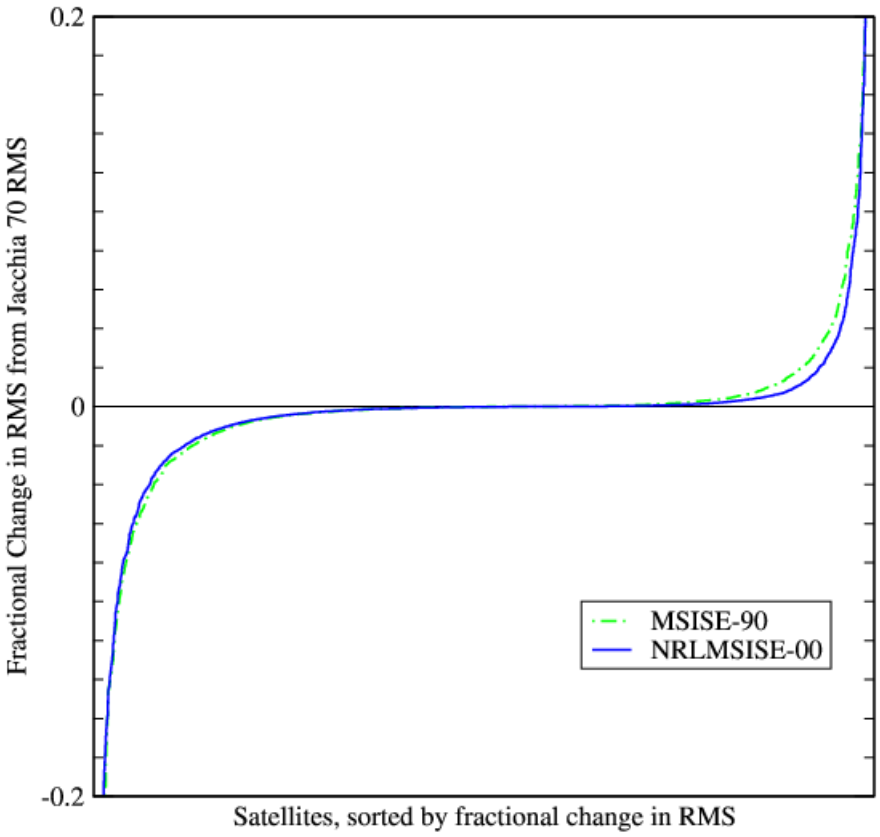

Figure 6: Fractional change in unweighted RMS for differential correction by satellite for the lowsats set, sorted by satellite in order of fractional change.

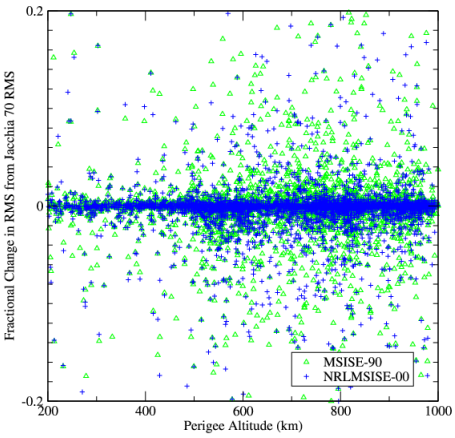

(a) Perigee altitude

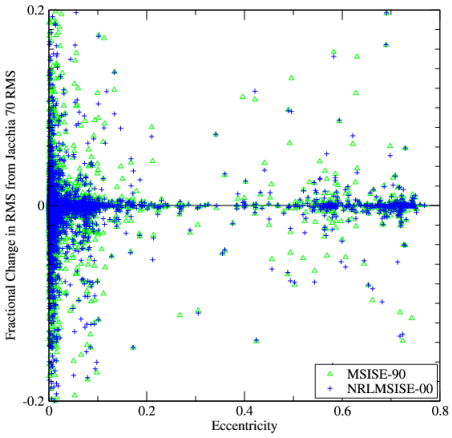

(b) Eccentricity

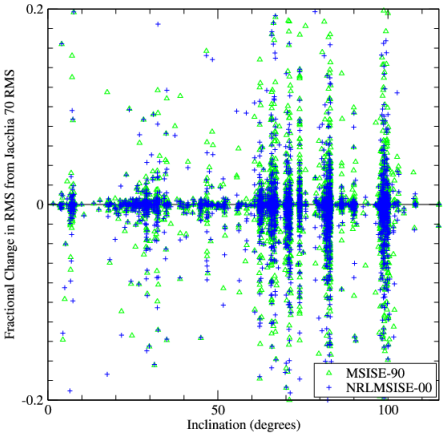

(c) Inclination

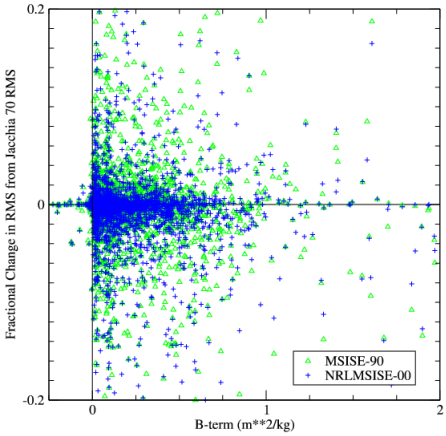

(d) Ballistic coefficient

Figure 7: Fractional change in unweighted RMS in lowsats differential correction plotted against various satellite parameters.

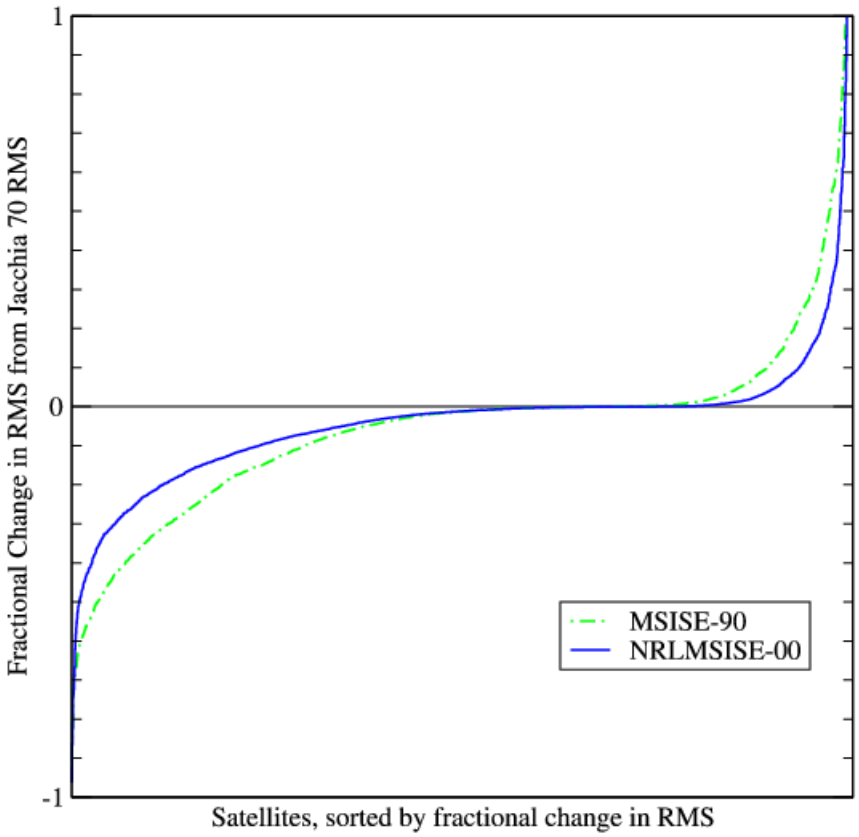

Figure 8: Fractional change in unweighted RMS for orbit propagation by satellite for the lowsats set, sorted by satellite in order of fractional change.

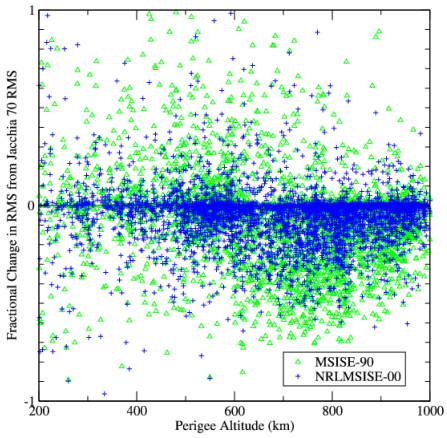

(a) Perigee altitude

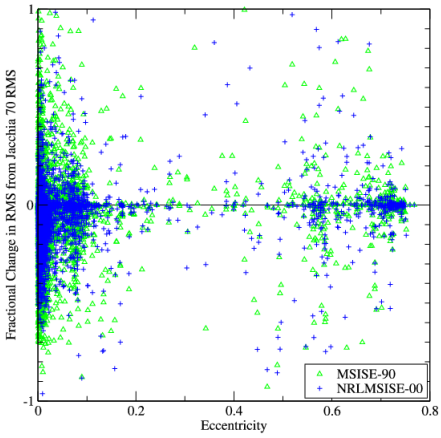

(b) Eccentricity

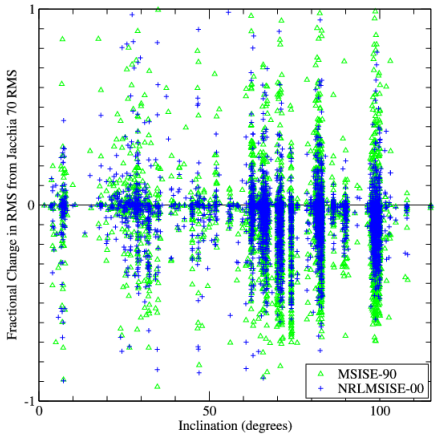

(c) Inclination

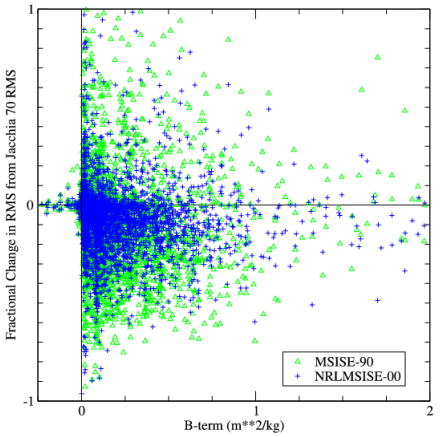

(d) B term

Figure 9: Fractional change in unweighted RMS for orbit propagation by satellite for the lowsats set, plotted against various satellite parameters.

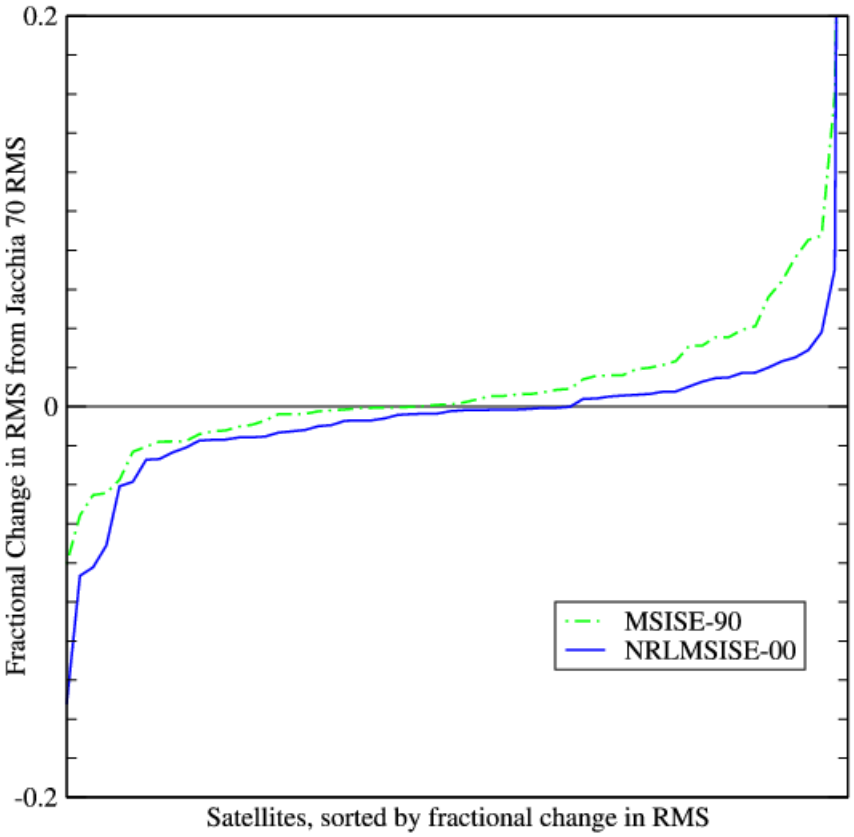

Figure 10: Fractional change in unweighted RMS in differential correction by satellite for the HASDM set, sorted in order of fractional change.

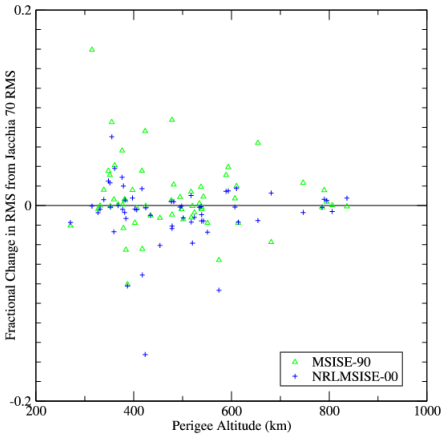

(a) Perigee altitude

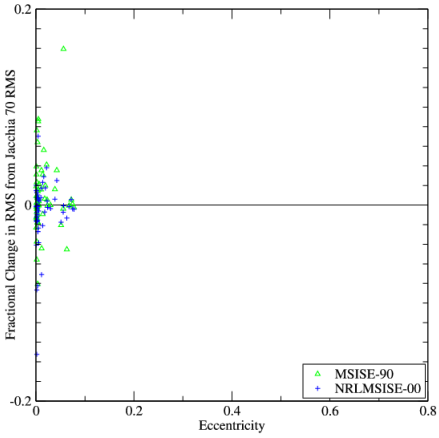

(b) Eccentricity

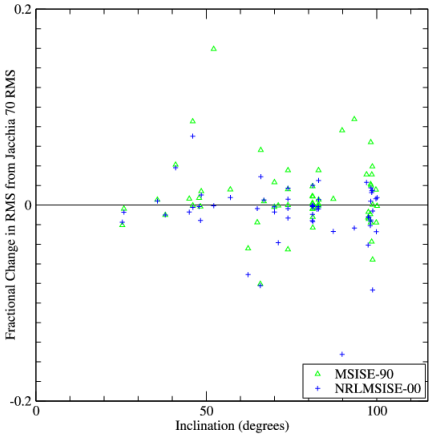

(c) Inclination

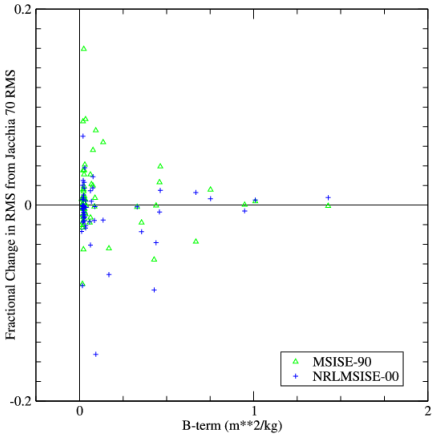

(d) B term

Figure 11: Fractional change in unweighted RMS in HASDM differential correction plotted against various satellite parameters.

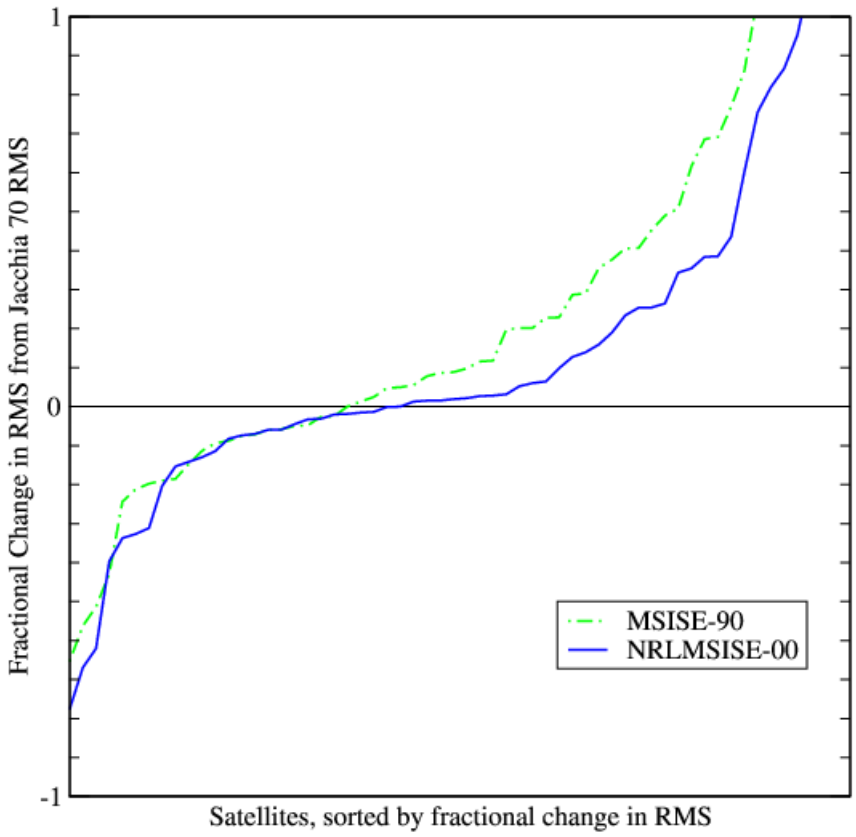

Figure 12: Fractional change in unweighted RMS for orbit propagation by satellite for the HASDM set, sorted in order of fractional change.

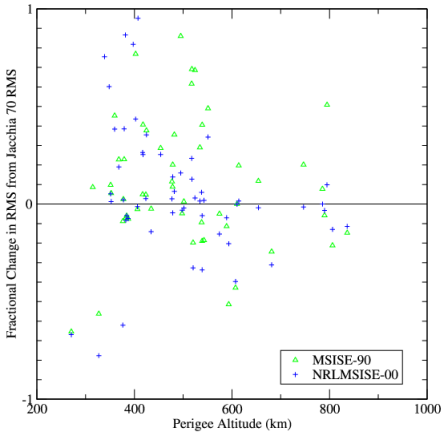

(a) Perigee altitude

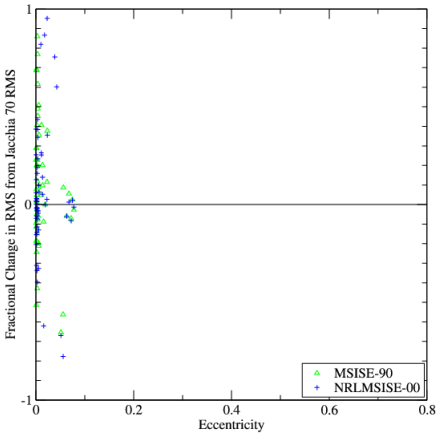

(b) Eccentricity

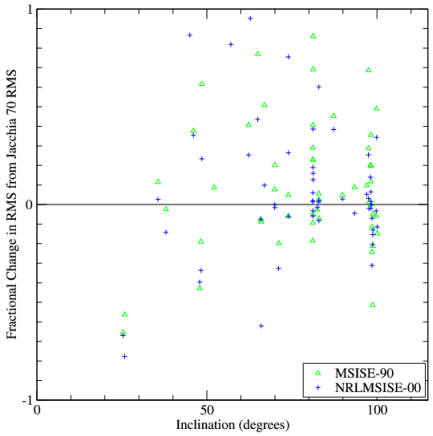

(c) Inclination

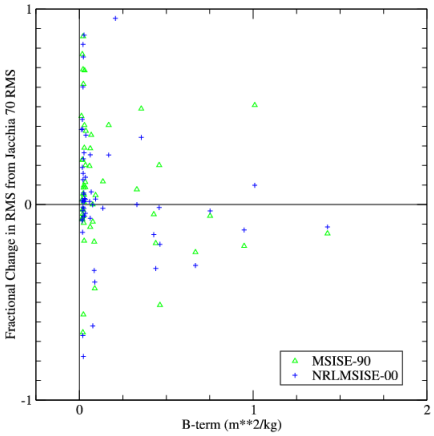

(d) B term

Figure 13: Fractional change in unweighted RMS for orbit propagation by satellite for the HASDM set plotted against various satellite parameters.

ONE DAY ORBIT-TO-ORBIT COMPARISON TEST

The atmospheric models may be compared by the relative predictive power of orbits determined with each. Specifically, we determined the orbits using each of three models and observations over a period of time ending (RST) at 1999-10-01 00:00:00 for the lowsats set and at 2001-02-15 00:00:00 for the HASDM set. Then, we redetermined the orbits 24 hours later, including new observations during that additional day. Finally, we propagated each of these determined orbits to the later RST and compared those positions. Thus, we have an orbit-to-orbit comparison. In our test, we included only those satellites that updated in all cases. For the lowsats, the total number of such satellites included is 4423; for HASDM, all 60 satellites updated.

This relative position vector is best presented in the normal, in-track, cross-track coordinate system (NTW) (Ref. 7). As one might suspect, most of the error is to be found in the in-track direction (Fig. 14(a)), though there can be significant error in the other directions (Figs. 14(b), 14(c)) as well. The figures show the distribution of displacement errors for each of the three axes for each of the three density models. The latter two are almost identically distributed for all three density models, and are very symmetric around zero. The distribution is computed by stepping every two meters, finding how many satellites were within a 10 meters of that value (5 meters for cross track and normal), and dividing by the total population times 10 (5) meters. It thus represents an approximate probability distribution.

To summarize, the means and standard deviations of each component for each drag model in the lowsats tests are given in Table 3. The distance between the two predicted values gives a scalar

	Normal	In-track	Cross-track
J70 mean	29.8	493.5	−0.8
J70 std. dev.	1902.4	16592.0	748.8
M90 mean	34.1	166.9	−11.8
M90 std. dev.	1941.1	16588.2	820.0
N00 mean	40.5	172.1	−11.8
N00 std. dev.	1950.5	16534.3	814.4

Table 3: Mean and standard deviation from orbit-to-orbit test for each drag model in the lowsats set. Units are meters.

summary of the error for each satellite in each density model.

Approximately 0.25% of the lowsats set had very high errors, over 10 km, for each of the density models. The most prominent among these, for J70 and M90, was satellite 25228, a Russian rocket body. This was because it decayed in mid-October 1999, shortly after the period that we studied. At the time of study, it was on a reentry trajectory, and its predictability was poor. One could reasonably expect that this would present a severe test of the drag modeling, and indeed, the results obtained showed the one day propagation error to be 2231 km for both J70 and M90. In contrast, the N00 value is 568 km. While too large to be useful, this gives some indication that N00 is better able to handle reentering satellites. In any case, it has been excluded from all the results above.

Other satellites which had large errors were not in obvious difficult trajectories, but still some errors were over 100 km. While these were small in number, the large magnitude significantly skews the mean and standard deviation position error.

The same test was performed on the HASDM set. Because there are so few satellites in this set, it does not lend itself to a probability density or histogram plot, so we simply summarize the results numerically in Table 4.

CONCLUSIONS

In this paper, we examined the relative accuracy for orbit determination and propagation of three atmospheric density models, using two sets of data: all the cataloged satellites with perigee below

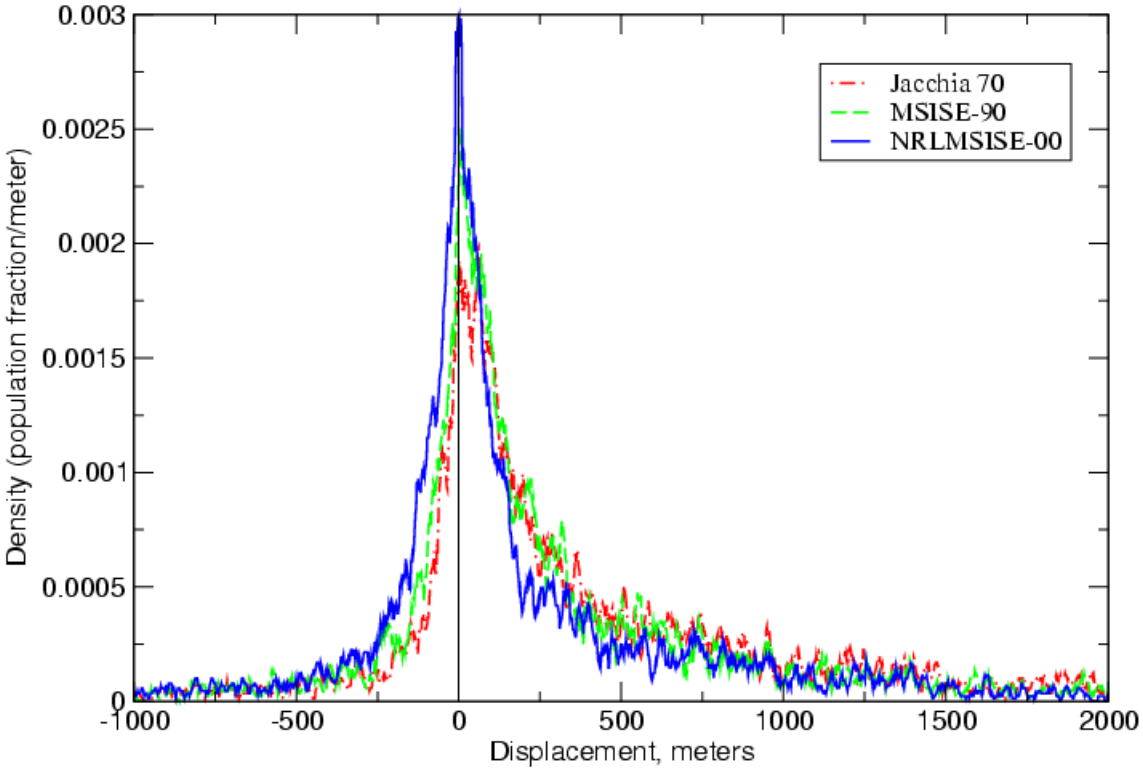

(a) In-track error

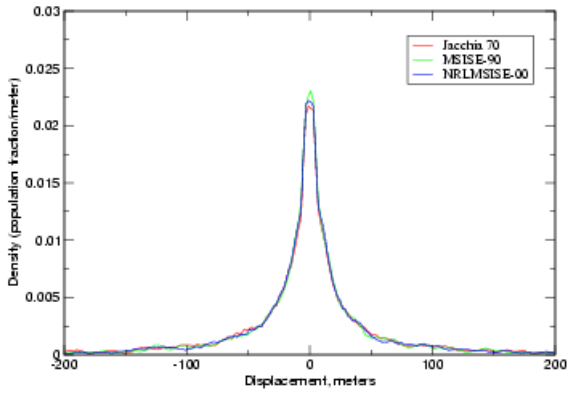

(b) Cross-track error

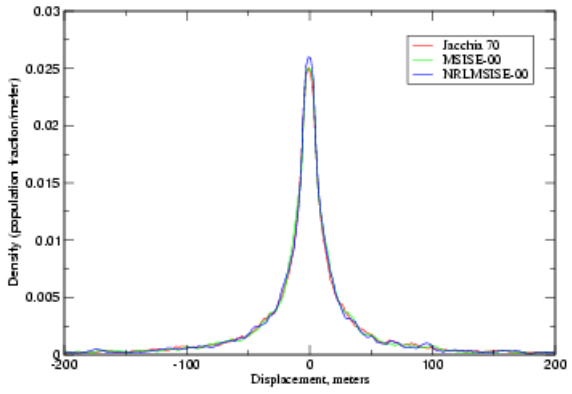

(c) Normal error

Figure 14: Distribution of errors in NTW frame of propagated day-old solution relative to newer solution for lowsats (1999) set.

	Normal	In-track	Cross-track
J70 mean	−16.4	1365.8	−0.2
J70 std. dev.	34.2	2552.1	21.6
M90 mean	−7.4	−7.4	8.3
M90 std. dev.	37.8	2224.4	59.0
N00 mean	−12.6	393.1	3.9
N00 std. dev.	42.4	2128.4	42.0

Table 4: Mean and standard deviation from orbit-to-orbit test for each drag model in the HASDM set. Units are meters.

1000 km, approximately 4500 satellites, and the HASDM calibration set of 60 satellites. In the majority of the tests performed, the MSIS-class models, led by NRLMSISE-00, demonstrate an improvement over the Jacchia model. However, it should be noted that this improvement overall is generally very small in light of the variations of the data and that, for the test where Jacchia proved better, the differences were also very small. In addition, individual satellites can show marked differences, with any of the three models showing the best results. Also, there was no evidence found to show that one model is better for any subset of the orbital regime, though this deserves more investigation. In the end, there is no single model which stands out as demonstrably superior over any other. There is hope, however, that the work currently underway on the implementation of the dynamic NRLMSISE-00 model will change this picture.

ACKNOWLEDGEMENTS

We thank Stefan Thonnard and Andy Nicholas for help with the MSIS model and suggestions on design and interpretation of the tests described. MSIS 90 was previously incorporated into SPeCIAL-K by Alan Segerman and Harold Neal.

REFERENCES

[1] Alan E. Hedin. MSIS-86 thermospheric model. *J. Geophys. Res.*, 92:4649–4662, 1987.

[2] L. G. Jacchia. New static models of the thermosphere and exosphere with empirical temperature models. Technical Report 313, Smithsonian Astrophysical Observatory, 1970.

[3] J. M. Picone, A. E. Hedin, D. P. Drob, and A. C. Aikin. NRLMSISE-00 empirical model of the atmosphere: Statistical comparisons and scientific issues. *J. Geophys. Res.*, 107(A12):1468, 2002.

[4] Alan E. Hedin. Extension of the MSIS thermosphere model into the middle and lower atmosphere. *J. Geophys. Res.*, 96:1159–1172, 1991.

[5] National Technical Information Service, Springfield, Virginia. *U.S. Standard Atmosphere*, 1976. (Product Number: ADA-035-6000); `http://nssdc.gsfc.nasa.gov/space/model/atmos/us_standard.html`.

[6] S. Knowles, M. Picone, S. Thonnard, A. Nicholas, K. Dymond, and S. Coffey. Applying new and improved atmospheric density determination techniques to resident space obect prosition prediction. In *Advances in Astronautics*, San Diego, CA, August 2001. American Astronautical Society, Univelt, Inc. AAS 01–426.

[7] David A. Vallado. *Fundamentals of Astrodynamics and Applications*. McGraw-Hill, New York, 1997.

[8] Harold L. Neal, Shannon L. Coffey, and Steve Knowles. Maintaining the space object catalog with special perturbations. In F. Hoots, B. Kaufman, P. Cefola, and D. Spencer, editors, *Astrodynamics 1997 Part II*, volume 97 of *Advances in the Astronautical Sciences*, pages 1349–1360, San Diego, CA, August 1997. American Astronautical Society. AAS 97–687.

[9] William H. Press, Brian P. Flannery, Saul A. Teukolsky, and William T. Vetterling. *Numerical Recipes in FORTRAN: The Art of Scientific Computing*. Cambridge University Press, 1992.